

Regular and chaotic vibrations in the rub impact model of a Jeffcott rotor with a fractional restore force

Grzegorz Litak¹ and Jerzy T. Sawicki²

¹ Department of Applied Mechanics, Technical University of Lublin, Nadbystrzycka 36, PL-20-618 Lublin, Poland

² Cleveland State University, Department of Mechanical Engineering, Cleveland, OH 44115, USA

Received: date / Revised version: date

Abstract. We study the solutions and bifurcations of the Jeffcott rotor with a rubbing effect. The model of horizontal rotor possesses such nonlinear effects as inertia, dry friction, and contact loss between the rotor and stator. By the exceeding of the rotor-stator radius clearance, the rotor can penetrate into the limiting rubbers with a fractional power in the restore force. The system response is analyzed by a bifurcation diagram. The specific cases are additionally clarified by means standard methods and quantified by the test 0-1 which is sensitive to chaotic behaviour.

Pacs: 05.45.Ac, 46.55.+d, 05.45.Gg

1 Introduction

The detection of rotor-to-stator rubbing based on vibration signatures is very important for both manufacturers and operators of rotating machinery. With the increase of machinery operating speed and efficiency, the rub-impact of stator and rotor is a common malfunction that may lead to a catastrophic failure. It has been well recognized that under certain conditions rotating machinery exhibit vibrations which have chaotic content, i.e., present unpredictable behavior. Such behavior is driven by the existence of nonlinearities in the system which could have

many roots, and one of them is interaction of the rotating and stationary components [1–5]. A great deal of research has been published in technical literature on the nonlinear dynamics of a rotor rubbing and/or impacting. Muszynska provided comprehensive review of the earlier publications on rub phenomena and discussed the major physical phenomena that occur during rubbing [5].

Goldman and Muszynska [4] used perturbation theory and numerical simulation to explore parameter regimes, in which the rub-related vibration becomes quasi-periodic and even chaotic. Adams and Abu-Mahfouz [6] numeri-

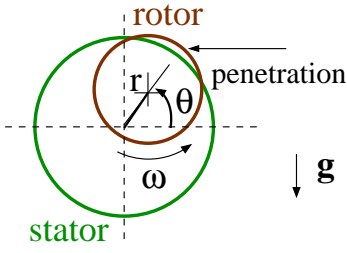


Fig. 1. The schema of a Jeffcott rotor with a rubbing effect, note that the stator-rotor clearance can be exceeded. We assume the restore force with a fractional power of the penetration depth.

cally explored the routes to chaos in several rotor models including a rub/impact model. Chaotic motion was also observed in experiments [7].

The mathematical model for this system has been originally proposed by Beatty [8]. Its similar versions were widely used to discuss bifurcation and chaotic motions including thermo-mechanical effects and experimental results analysis [9–14].

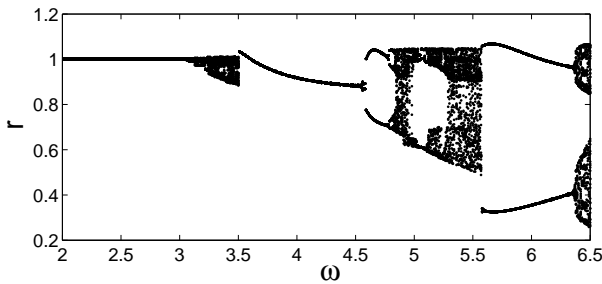


Fig. 2. Bifurcation diagram of the system obtained through continuation of solution during the quasistatic increase of rotational velocity ω .

2 The model and its dynamical response

In the present note we followed the basic rub-impact model assumptions [5, 7]. In addition, we consider that contact dynamics is dependent on exceeding of the rotor-stator radial clearance through the limiting rubbers by assuming a fractional power in the restore force.

The non-dimensional equations of motion in terms of polar coordinates (r, θ) see Fig. 1) be written [14]

$$\begin{aligned} \ddot{r} + 2\zeta\dot{r} + (1 - \dot{\theta})r &= u\omega^2 \cos(\omega t - \theta) - g' \sin(\theta) - f_r, \\ r\ddot{\theta} + 2(\dot{r} + \zeta r)\dot{\theta} &= u\omega^2 \sin(\omega t - \theta) - g' \cos(\theta) - f_t. \end{aligned} \quad (1)$$

The above model includes the gravitation, inertial and contact effects. The contact forces radial thrust f_r and the transverse friction forces f_t can be expressed:

$$\left. \begin{aligned} f_r &= \omega_s (r - 1)^{3/4} \\ f_t &= \mu f_r \end{aligned} \right\} \text{if } r \geq 1 \text{ otherwise } f_r = f_t = 0. \quad (2)$$

The non-dimensional system parameter were chosen as $u = 0.125$, $\zeta = 0.6$, $g' = 1.962$, $\mu = 0.2$, and $\omega_s = 240$ [14], while ω was changing through the interval values $\omega \in [2, 6.5]$. In Fig. 2a we show the bifurcation diagram indicating series of system bifurcation. Note that the character of the solution changes several times. Following these changes one can easily distinguish the regular and chaotic motion in terms of stroboscopic points (projected to r axis with the frequency ω) wide distributions. The bifurcations appeared in this system have a direct analogy to the stick and slip vibration of a spring-mass system on the transportation belt [15]. Generally, such nonsmooth systems are not easy to analyze as dimensionality of system are

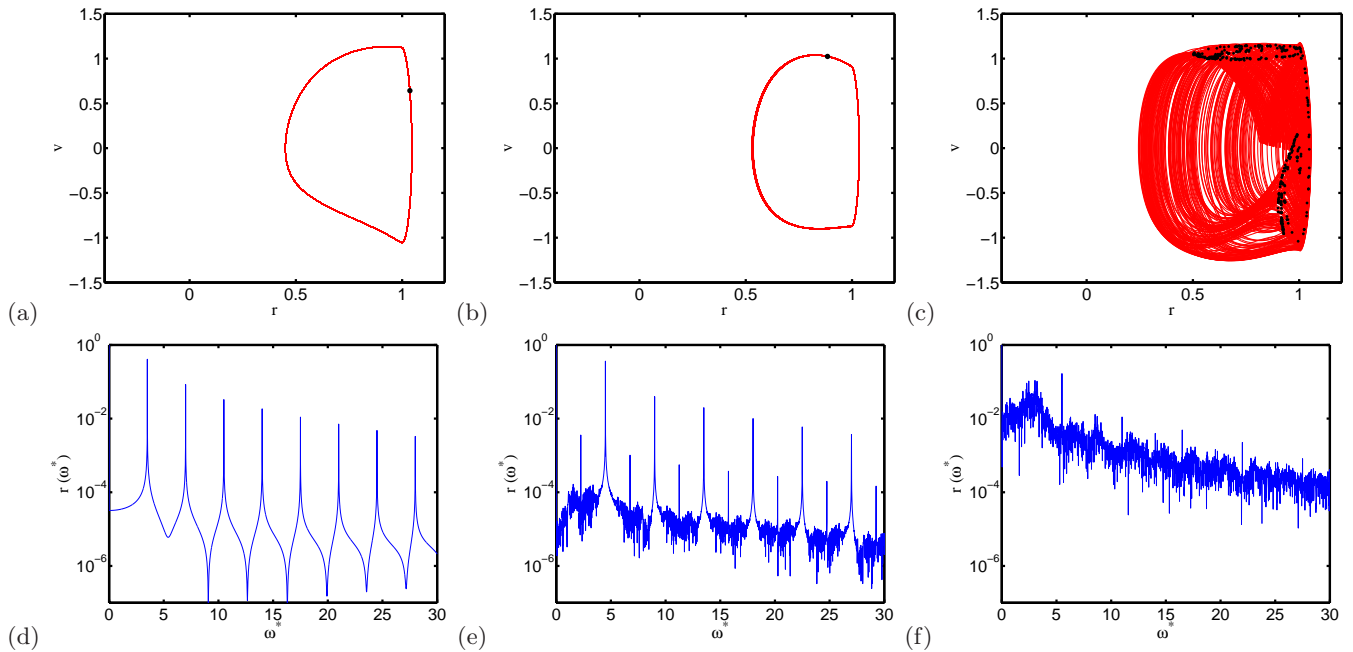


Fig. 3. (color online) In the upper panel – the phase portraits (with red lines) and Poincaré maps (with black points) (a)–(c) for the radial coordinate r ($v = \dot{r}$); in the lower panel – the corresponding Fourier transforms $r(\omega^*)$ (d)–(f). Rotational velocity: (a),(d) $\omega = 3.6$; (b),(e) $\omega = 4.5$; (c),(f) $\omega = 5.5$.

changing with time. The impacts or contact-loss phenomena provides additional complications [16]

For further investigations we focus on the characteristic cases of rotational velocity $\omega = 3.6, 4.5$ and 5.5 . In Fig. 3a-f, we show the phase portraits, Poincaré maps and Fourier spectra of the radial coordinate r response. One can see the regular vibrations reflected as single loops of the phase portrait and localized (black) points of Poincaré maps Fig. 3a and b (for $\omega = 3.6$ and 4.5 , respectively) while the chaotic motion represented by the strange attractor with a complicated topology of the phase portrait in Fig. 3c. In the lower panel of Fig. 3, these expectations are confirmed by showing the corresponding Fourier spectra. Interestingly, for $\omega = 4.5$ (Fig. 3e) the Fourier spectrum is not so clear as in Fig. 3d ($\omega = 3.6$). This in-

dicates the important component in phase θ oscillations at the vicinity of the period doubling bifurcation (see Fig. 2). Further investigation could show the quasiperiodic nature of this solution. On the other hand the last figure of the Fourier spectrum ($\omega = 5.5$, Fig. 3f) is definitely of continuous distribution as expected for a chaotic solution. Figures 3a-f are consistent with the bifurcation diagram (Fig. 2). Note that the case $\omega = 3.6$, represented in Fig. 2 by a point, is just above the smeared dark region. The solution of $\omega = 4.5$ must be of a similar type, while the solution of $\omega = 5.5$ (Fig. 2) is located in a dark region and could be identified as a chaotic solution.

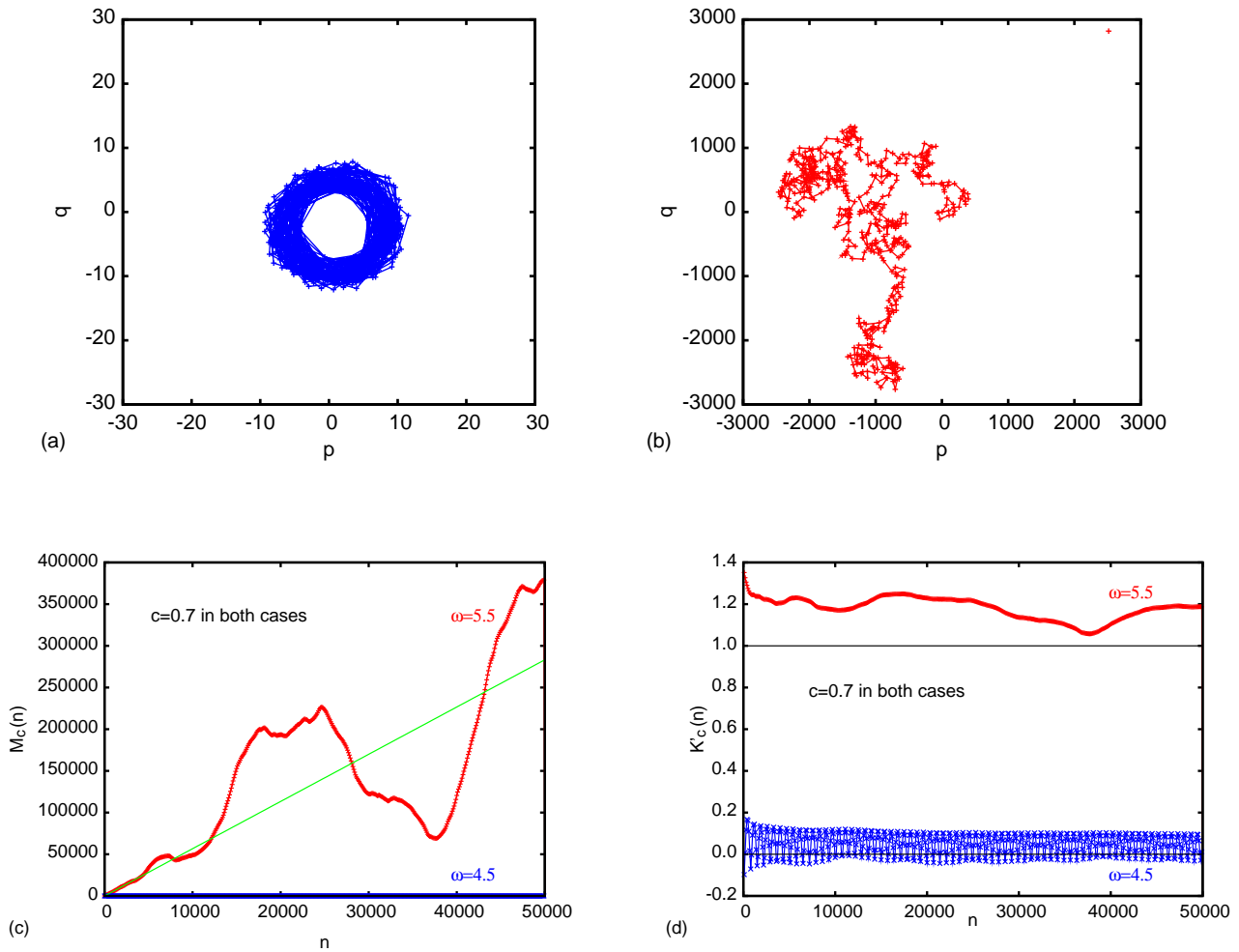


Fig. 4. p - q phase plots for $\omega = 4.5$ (a) and 5.5 (b). The length of time series was $n_{max} = 54200$ ($c = 0.7$). Note, differences in the axis scale (a,b). Total mean square displacement $M_c(n)$ versus sampling time n for $c = 0.7$ (c), and the corresponding parameter $K'_c(n)$ (d). The inclined straight line (green) in Fig. 4c reflects the linear growth the total mean square displacement obtained by fitting by least squares to $M_c(n)$.

3 The 0-1 test

The 0-1 test, invented by Gottwald and Melbourne [17, 18], can be applied for any system of a finite dimension but it is basing on the statistical properties of a single coordinate only. As related to the universal properties of the dynamical system like spectral measures, it can dis-

tinguish chaotic system from regular one. In particular, the 0-1 test, has an advantage against the frequency spectrum as it provides information about the dynamics in single parameter value, similarly to Lyapunov exponent. However, the Lyapunov exponent is difficult to estimate in any nonsmooth systems [20]. The present model (Eq. 1) including friction and contact loss effects is represent-

ing this class of nonsmooth system. Therefore the 0-1 test can provide the suitable algorithm to identify the chaotic solution [21–24].

To start the analysis, we discretize the investigated time series $r(t) \rightarrow r(i)$ using the characteristic delay time δt equal to one quarter of the revolution time $2\pi/\omega$. This roughly indicates vanishing of the mutual information [21, 25]. Starting from one of the initial map coordinate $r(i)$ we defined defining new coordinates $p(n)$ and $q(n)$ as

$$\begin{aligned} p(n) &= \sum_{j=0}^n \frac{(r(j) - \bar{r})}{\sigma_r} \cos(jc), \\ q(n) &= \sum_{j=0}^n \frac{(r(j) - \bar{r})}{\sigma_r} \sin(jc), \end{aligned} \quad (3)$$

where \bar{r} denotes the average value of r while σ_r its standard deviation. Note that $q(n)$ is a complementary coordinate in the two dimensional space. Here the constant $c = 0.7$ has been chosen arbitrary. Note that starting from bounded coordinate $x(i)$ we build new series of $p(n)$ which can be either bounded or unbounded depending on dynamics of the examined process. This effect has been illustrated in Figs. 4a,b for $\omega = 4.5$ and $\omega = 5.5$, respectively. Note, Fig. 4a shows a characteristic small radius circular pattern while Fig. 4b resembles unbounded random walks. The statistical properties are determined by the scale difference in the corresponding $p - q$ phase diagrams.

The total mean square displacement

$$\begin{aligned} M_c(n) &= \lim_{N \rightarrow \infty} \frac{1}{N} \sum_{j=1}^N [(p(j+n) - p(j))^2 \\ &+ (q(j+n) - q(j))^2], \end{aligned} \quad (4)$$

Note that in our two characteristic cases ($\omega = 4.5$ (Fig. 4a) and 5.5 (Fig. 4b)) we observe clear growth of $M_c(n)$ (Fig. 4c). To show this growth plot its linear fit by least squares (see the strait inclined line in Fig. 4c).

The asymptotic growth can be easily characterized by the corresponding ratio $K'_c(n)$

$$K'_c(n) = \frac{\ln(M(n))}{\ln n}. \quad (5)$$

This parameter has been also shown in Fig. 4d. In the limit of a very long time $n \rightarrow \infty$ (in practice $n = n_{max} = 54200$ while $N = 4000$) we obtained $K'_c = 0.14$ for $\omega = 4.5$ and $K'_c = 1.19$ for $\omega = 5.5$ ($c = 0.7$). Note, our choice of n_{max} and N limits (in Eqs. 4 and 5) is consistent with that proposed by Gottwald and Melbourne [19] $N, n_{max} \rightarrow \infty$ but simultaneously N should be about $n_{max}/10$.

It is important to note that the parameter c acts like a frequency in a spectral calculation, (see Eq. 3). If it is badly chosen, resonates with one rotational frequency or its multiple (see Figs. 3d-f). In the 0-1 test regular motion would yield a ballistic behavior in the (p, q) -plane and the corresponding $M_c(n)$ results in an asymptotic growth rate even for regular system. The disadvantage of the test, its strong dependence on the chosen parameter c , could be overcome by a proposed modification. Gottwald and Melbourne [19, 22, 23] suggest to take randomly chosen values of c and compute the median of the belonging K_c -values.

Consequently, the new covariance formulation

$$K_c = \frac{\text{cov}(\mathbf{X}, \mathbf{M}_c)}{\sqrt{\text{var}(\mathbf{X})\text{var}(\mathbf{M}_c)}}, \quad (6)$$

where vectors $\mathbf{X} = [1, 2, \dots, n_{max}]$, and $\mathbf{M}_c = [M_c(1), M_c(2), \dots, M_c(n_{max})]$.

In the above, the covariance $\text{cov}(\mathbf{x}, \mathbf{y})$ and variance $\text{var}(\mathbf{x})$, for arbitrary vectors \mathbf{x} and \mathbf{y} of n_{max} elements, and the corresponding averages \bar{x} and \bar{y} respectively, are defined

$$\begin{aligned} \text{cov}(\mathbf{x}, \mathbf{y}) &= \frac{1}{n_{max}} \sum_{n=1}^{n_{max}} (x(n) - \bar{x})(y(n) - \bar{y}), \\ \text{var}(\mathbf{x}) &= \text{cov}(\mathbf{x}, \mathbf{x}). \end{aligned} \quad (7)$$

Finally, the median is taken of K_c -values (Eq. 6) corresponding to 100 random values of $c \in (0, \pi)$. Such an average K -value can be now estimated for various rotational frequency ω . The results presented in Fig. 5 show that for chaotic regions $K \geq 0.8$ while for regular regions K is very close to 0. The intermediate cases signals the vicinity to bifurcation points or very long transients.

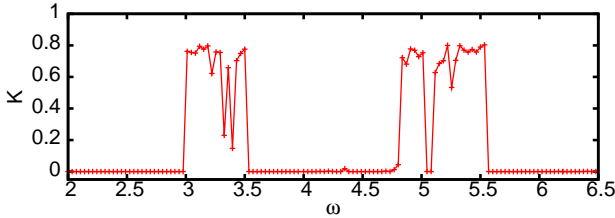


Fig. 5. Estimated average K parameter of the test 0-1 (calculated using Eqs. 4 & 6) for 100 random values $c \in (0, \pi)$ at each ω point ($N = 4000$ while $n_{max} = 50000$).

4 Conclusions

In summary, we would like to write that our rub impact model show complex self-excited vibrations. Our development to the model included the fractional power law of the restore force once the rotor exceeded the limiting barriers. Motivated by the machining process models [22] we used

the fixed exponent 0.75 of the restore force, but the actual value should be dependent on the material and thermal properties of contacting rotor-stator parts. Finally, it is also important note that due to the nonsmoothness in the examined model a relevant quantitative characterization (via Lyapunov exponents) of responses is difficult. The alternative approach should involve more sophisticated time-series approaches with a suitable embedding [25].

Acknowledgements

GL gratefully acknowledges the support of the Polish National Science Center under the grant No. 2012/05 /B/ST8/00080.

References

1. F. Ehrich, *J. Vibr. Acoust.* **114**, 93 (1992).
2. D. Kraker, M.T.M. Crooijmans, D.H. Campen, *Proc. IMechE. C* **284**, 297 (1988).
3. J. Padovan, F.K. Choy, F.K., *J. Turbomachinery* **108**, 527 (1987).
4. P. Goldman, A. Muszynska, *J. Vibr. Acoust. Vol.* **116**, 541 (1994).
5. A. Muszynska, *Shock Vibr. Digest* **21**, 3 (1989).
6. M.L. Adams, I.A. Abu-Mahfouz, I. A., in *Proceedings of The Fourth Int. Conf. on Rotor Dynamics*, Chicago, IL, 29 (1994).
7. H.C Piccoli, H.I. Weber, *Nonlin. Dyn.* **16**, 55 (1998)
8. R.F. Beatty, *J. Vib. Acoust.* **107**, 151 (1985).

9. J.T. Sawicki, J. Padovan, R. Al-Khatib, *Int. J. Rotating Machinery* **5**, 295 (1999).
10. J.T. Sawicki, A. Montilla-Bravo, Z. Gosiewski, *Int. J. Rotating Machinery* **9**, 295 (2003).
11. J.T. Sawicki, Technical Report, GE CRDC, Schenectady 2000, unpublished.
12. F. Chu, Z. Zhang, *J. Sound Vib.* **210**, 1 (1998).
13. F. Chu, W. Lu, Experimental observation of nonlinear vibrations in a rub-impact rotor system. *J. Sound Vib.* **283**, 621 (2005).
14. J.-O. Aidanää, in *Proc. of The 10th Int. Sym. on Transport Phenomena and Dynamics of Rotating Machinery*, Honolulu, Hawaii, March 07-11, (2004).
15. K. Popp, P. Stelter *Phil. Trans. Roy. Soc. London* **332**, 89 (1990).
16. E.V. Karpenko, M. Wiercigroch, E.E. Pavlovskaja, M.P. Cartmell, *Int. J. Mech. Sciences* **44**, 475 (2002).
17. G.A. Gottwald, I. Melbourne, *Proc. R. Soc. Lond. A* **460**, 603 (2004).
18. G.A. Gottwald, I. Melbourne, *Physica D* **212**, 100 (2005).
19. G.A. Gottwald, I. Melbourne, *SIAM J. App. Dyn. Syst.* **8**, 129 (2009).
20. A. Wolf, J.B. Swift, H.L. Swinney, J.A. Vastano, *Physica D* **16**, 285 (1985).
21. G. Litak, A. Syta, M. Wiercigroch, *Chaos, Solitons & Fractals* **40**, 2095 (2009).
22. G. Litak, S. Schubert, G. Radons, *Nonlinear Dyn.* **69**, 1255 (2012).
23. B. Krese, E. Govekar, *Nonlinear Dyn.* **67**, 2101 (2012).
24. G. Litak, D. Bernardini, A. Syta, G. Rega, A. Rysak, *Eur. Phys. J. Special Topics* **222**, 1637 (2013).
25. H. Kantz H., Schreiber T. *Non-linear Time Series Analysis*, (Cambridge University Press, Cambridge 1997).